Journal of Biomechanics 92 (2019) 126–136

Contents lists available at ScienceDirect

Journal of Biomechanics

journal homepage: www.elsevier.com/locate/jbiomech
www.JBiomech.com

Esophageal stress softening recovery is altered in STZ-induced diabetic rats

Hongbo Jiang [a,b,c], Jingbo Zhao [a,c], Donghua Liao [c], Guixue Wang [a,*], Hans Gregersen [d]

[a] GIOME and the Key Laboratory for Biorheological Science and Technology of Ministry of Education, Bioengineering College of Chongqing University, Chongqing 400044, China
[b] Yiducloud (Chongqing) Technology Co., Ltd., Chongqing 400044, China
[c] Giome Academia, Department of Clinical Medicine, Aarhus University, 8200 Aarhus N, Denmark
[d] GIOME, Department of Surgery, The Chinese University of Hong Kong, Hong Kong

ARTICLE INFO

Article history:
Accepted 27 May 2019

Keywords:
Cyclic loading
Stored energy recovery
Esophageal remodeling
KCl activation
Experimental diabetes
Rat model

ABSTRACT

This study investigated stress softening recovery in intact, separated muscle and mucosa-submucosa esophageal tubes in streptozotocin-induced diabetic rats. Fifteen Wistar rats were made diabetic (DM group) by intraperitoneal injection of 50 mg kg^{-1} streptozotocin and another 11 rats served as Sham group by injection of saline. All rats survived for 8-weeks. Three series of inflation-deflation loadings at luminal pressure levels of 0.5, 1.0 and 2.0 kPa were carried out on different esophageal tubes. Five distension cycles on each pressure level were done in Ca^{++}-free Krebs solution before and after KCl activation in Ca^{++}-containing Krebs solution. The wall stiffness and stored energy recovery were compared between two groups. The stiffness was biggest in the DM group for the intact tube at pressure 0.5 kPa ($P < 0.01$) and for the muscle tube at all pressure levels ($P < 0.05$). Energy recovery induced by stress softening and stiffness loss recovery were significantly smaller in the DM group than in the Sham group for the intact esophagus and separated tubes at all pressure levels ($P < 0.05$, $P < 0.01$). In conclusion, the reversible stress softening and passive stiffness recovery were altered in STZ-induced diabetic rats. This study fills a gap in the knowledge about diabetes-induced esophageal remodeling.

1. Introduction

Diabetes is a chronic disease requiring lifelong medical attention. The most recent data from the International Diabetes Federation indicated that diabetes affected 451 million people worldwide in 2017, a number that is expected to grow to 693 million by 2045 (Cho et al., 2018). Therefore, diabetes is a major public health problem. The global healthcare expenditure on people with diabetes was estimated to be USD 850 billion in 2017 (Cho et al., 2018).

Esophageal sensory-motor dysfunction is quite common in diabetic patients (Zhao and Gregersen, 2016). Studies have clearly demonstrated remodeling of esophageal structure and biomechanical properties during development of diabetes (Frokjaer et al., 2007, 2012; Yang et al., 2004, 2006; Zhao et al., 2007a). The remodeling may relate to esophageal sensory-motor dysfunction in diabetes (Zhao and Gregersen, 2016). To the best of our knowledge, no study has been reported on esophageal stress-softening characteristics in diabetes. In order to obtain a comprehensive understanding of diabetic induced remodeling of esophageal biomechanical properties, time history related changes in esophageal stress softening and its reversible characteristics during the development of diabetes are needed.

Such study cannot be performed in humans; therefore, we have to do it in a relevant animal model. In our previous studies, we focused on the STZ-induced diabetic rat model (Yang et al., 2004, 2006). Furthermore, esophageal stress softening recovery after KCl activation has been demonstrated in normal intact and layered rat esophagus (Jiang et al., 2014, 2017). The adjustable passive stress and stiffness are believed to be recovered due to RhoA kinase (ROK)-dependent Ca^{2+} sensitization induced by KCl (Ratz et al., 2005). For comparability with previous studies, we adopted the STZ-induced diabetic rat model in the present study. The purpose of this study was to investigate the stress-softening properties of intact esophageal and of separated muscle and mucosa-submucosa tubes in STZ-induced diabetic rats. We hypothesized that esophageal stress softening recovery was inhibited during development of diabetes.

* Corresponding author at: State Key Laboratory of Mechanical Transmission, Key Laboratory for Biorheological Science and Technology of Ministry of Education, State and Local Joint Engineering Laboratory for Vascular Implants, Bioengineering College of Chongqing University, Chongqing 400044, China.
E-mail address: wanggx@cqu.edu.cn (G. Wang).

https://doi.org/10.1016/j.jbiomech.2019.05.042
0021-9290/

2. Materials and methods

2.1. Animals and groups

Twenty-six male Wistar rats (8 weeks old, weight 250–300 g) were included in this study. Fifteen rats were used in the diabetic group (DM) and 11 rats were used in the non-diabetic control group (Sham). Diabetes was induced by a single intraperitoneal injection of 50 mg kg^{-1} streptozotocin (STZ, Sigma-Aldrich, Denmark). The body weight and blood glucose level were measured at day 1, day 3, day 4, day 7, and weekly afterwards. Seven of the diabetic rats and 5 normal rats were used for intact esophagus test whereas 8 diabetic rats and 6 normal rats were used for the separated mucosa-submucosa and muscle tube test. Approval of the protocol was obtained from the Danish Committee for Animal Experimentation (2004-561-929).

2.2. Chemical solutions

Ca^{++}-containing Krebs solution (g L^{-1}): NaCl, 6.89; KCl, 0.35; $NaHCO_3$, 2.1; NaH_2PO_4, 0.12; $MgSO_4$, 0.144; $CaCl_2$–H_2O, 0.367; Ascorbic acid, 0.02 and Dextroglucose, 2.2.

Ca^{++}-free Krebs solution: same as the solution above without $CaCl_2$–H_2O and Dextroglucose but with EGTA (0.2 g L^{-1}).

All chemicals were purchased from Sigma-Aldrich, Inc.

2.3. Collection of specimens

At the end of the experiment of 8 weeks, the rats fasted overnight and were then anesthetized with subcutaneous injection of Hypnorm 0.05 mg kg^{-1} and Dormicum 0.025 mg kg^{-1}. The abdominal and thoracic cavities were opened and the whole esophagus was carefully dissected. The esophagus was cut at the proximal and distal ends (approximate 5 cm *in vivo* length) and transferred into an organ bath containing Ca^{++}-free Krebs solution (36–37 °C, 95% O_2 and 5% CO_2, pH = 7.4) to eliminate spontaneous contractile activity. After 20 min, the *in vitro* length of the esophagus was measured. A segment (3 cm) from the lower part of the esophagus was cut and used in the stress softening test (see later). For the testing of separated tubes, the intact esophageal tube was carefully separated into muscle and mucosa–submucosa tubes under microscopy (Jiang et al., 2017). Two rings (approximate 1 mm wide) were cut from the middle part of the different esophageal tubes after the stress softening test. The rings were immersed separately in small organ baths containing the Ca^{++}-free Krebs solution (36–37 °C) and were photographed at no-load state after 30 min for equilibration that was used for reference state determination. All specimens were saved in formalin for histological analysis after finishing the test.

2.4. Biomechanical test set-up

A tailor-made organ bath was designed for the intact (Jiang et al., 2014) and the separated (Jiang et al., 2017) esophageal tube experiments. The organ baths for the intact wall and the separated layer distention experiments are slightly different. The former contained only one distension channel whereas the latter had two parallel distension channels for simultaneous testing of the muscle and mucosa-submucosa tubes. The Krebs solution contained in the small chamber was maintained constant at 36–37 °C by circulating the water in the outer chamber using a peristaltic pump combined with a heater. The esophageal tubes were placed in the small organ bath containing Krebs solution. The two ends of each specimen were tied to cannulas separately with silk threads. The cannula at the proximal end was connected via a three-way tube to a syringe containing Krebs solution to apply luminal pressure using a pump (Genie Programmable Syringe Pump, World Precision Instrument, Stevenage, UK). A tube with a three-way connector was connected to a pressure transducer (Disposable Pressure Transducers, SCW MEDICATH LTD, Shenzhen, China) to record the inlet pressure. The other two cannulas at the distal end were connected to the pressure transducers to record the pressure inside the lumen of the segments. The diameter changes of the specimens were videotaped through a stereomicroscope (Olympus, Japan) by a CCD camera (Sony, Japan) and aligned to the pressure recordings. The system and data acquisitions were controlled using OpenLab software (GateHouse A/S, Denmark). The frequency of pressure data sampling was 10 Hz.

2.5. Biomechanical test protocol

The protocol is shown in Fig. 1. For the separated tube experiments, the muscle and mucosa-submucosa segments were tested simultaneously. Each segment was stretched to its *in vivo* length by adjusting the distance between the two cannulas. The tubular segments were subjected to the first test series (S1 series) of cyclic distension loadings (0.8 ml min^{-1}), up to pressure levels of 0.5, 1.0 and 2.0 kPa, respectively. For each pressure level, five inflation–deflation cycles were conducted. After 10 min rest, the segments were subjected to a second test series (S2 series) of similar loadings as in the S1 series. Afterwards, the Ca^{++}-free Krebs solution in the small organ bath was replaced with Ca^{++}-containing Krebs solution, and the specimens rested in the solution for 1 h to recover muscle tone. At the end of this period, the segments were distended to 1.0 kPa and volume inside the segments was maintained constant by closing the outlet. 10 ml KCl solution (110 mM L^{-1}, 36–37 °C) was added into the small organ bath to evoke contractile activity. KCl was washed out after 3 min by exchanging the solution with Ca^{++}-free Krebs solution. The pressure was zeroed to empty the segments. After 1 h rest in the Ca^{++}-free Krebs solution to eliminate muscle tone, the specimens were exposed to a third (recovery) test series (Re series) of cyclic loadings similar to those in the S1 and S2 series.

2.6. Stress–strain analysis

The outer diameters of the segments during distensions were measured from the recorded video images by a house-made subroutine. The outer circumferential length (C_{o-n}) and cross-sectional area (A_n) of the tissue rings at the no-load state were measured using SigmaScan image analysis software (Jandel Scientific, USA). The radius of the tissue rings at no-load state were calculated as:

The outer radius r_{o-n}:

$$r_{o-n} = \frac{C_{o-n}}{2\pi} \tag{1}$$

The inner radius r_{i-n}:

$$r_{i-n} = \sqrt{r_{o-n}^2 - \frac{A_n}{\pi}} \tag{2}$$

During each loading–unloading cycle, the strain and stress were denoted as:

Circumferential mid-wall green strain $E_{\theta\theta}$:

$$E_{\theta\theta} = \frac{\lambda_{\theta\theta}^2 - 1}{2} \tag{3}$$

where $\lambda_{\theta\theta} = \frac{r_{i-l}+r_{o-l}}{r_{i-n}+r_{o-n}}$ is the circumferential mid-wall stretch ratio, and

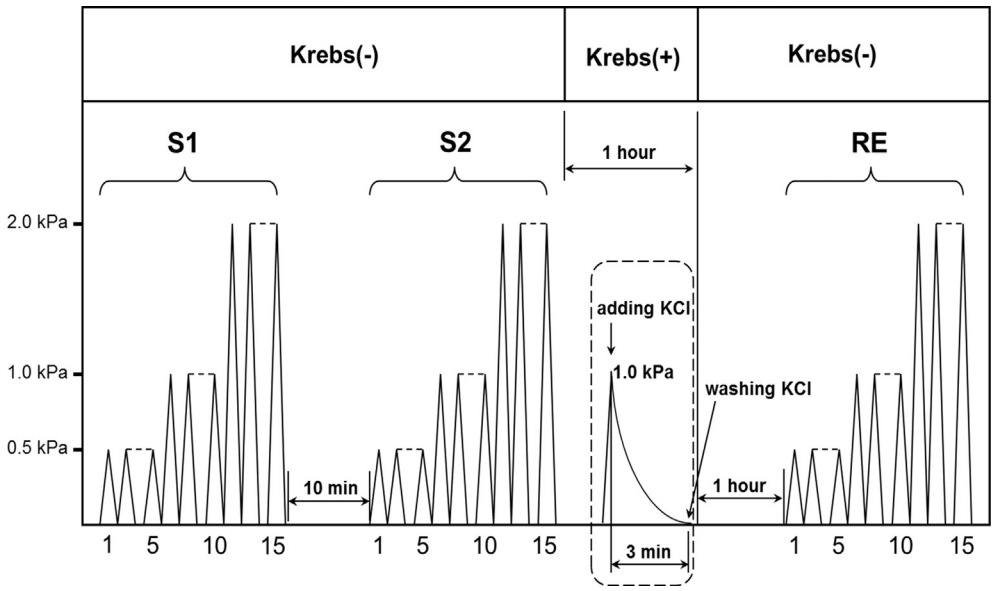

Fig. 1. Schematic diagram of the cyclic loading test protocol. Five inflation–deflation cycles of the S1 series were conducted up to maximum pressure levels of 0.5, 1.0 and 2.0 kPa in calcium-free medium (Krebs(−)). The S2 series was conducted 10 min after finishing S1. After S2 the testing specimens were incubated in calcium-containing solution (Krebs(+)) for 1 h. Then, the specimens were inflated to 1.0 kPa and activated by KCl for 3 min. After washing KCl out, the specimens were incubated in the Krebs(−) solution again for 1 h and the Re series was conducted.

$$r_{i-l} = \sqrt{r_{o-l}^2 - \frac{A_n}{\pi \lambda_{zz}}}, \qquad r_{o-l} = \frac{d_{o-l}}{2} \tag{4}$$

where $r_{i\text{-}l}$ and $r_{o\text{-}l}$ are the inner radius and the outer radius of the specimen at the loaded state, $d_{o\text{-}l}$ is the diameter of the specimen at the loaded state and λ_{zz} is the *in vivo* longitudinal stretch ratio. Circumferential Kirchhoff stress $S_{\theta\theta}$:

$$S_{\theta\theta} = \frac{\mathrm{Pr}_{i-l}}{h\,\lambda_{\theta\theta}^2} \tag{5}$$

where $h = r_{o\text{-}l} - r_{i\text{-}l}$ is the wall thickness and P is the intraluminal pressure at the loaded state.

2.7. Stress softening analysis

The stress softening was assessed by comparing the stored energy and elastic modulus at different maximum pressures of distension.

1) Stored energy evaluation (Jiang et al., 2014)

Stored energy in the esophageal tissues is reflected by the hysteresis loop area between the loading-unloading stress-strain curves. The area of each hysteresis loop was calculated by a MATLAB subroutine (R14, Mathworks, USA). For each specimen, every hysteresis loop area was normalized by the maximum hysteresis area during the whole test for eliminating variances caused by different specimens.

2) Wall stiffness estimation

To evaluate the stiffness of the intact and layered esophagus and the effect of diabetes on stiffness we estimated the wall stiffness at different stress levels of the intact layer, the mucosa-submucosa layer and the muscle layer at different maximum pressures of distension (Zhao et al., 2007b).

The stress-strain data were nonlinearly curve fitted using a uniaxial exponential stress-strain relation as follows.

$$S_{\theta\theta} = \left(S_{\theta\theta}^* + b\right) e^{a\left(E_{\theta\theta} - E_{\theta\theta}^*\right)} - b \tag{6}$$

where $S_{\theta\theta}$ is circumferential stress, $E_{\theta\theta}$ is circumferential strain, and $S_{\theta\theta}^*$ and $E_{\theta\theta}^*$ are the stress and the strain at an arbitrary point on the stress-strain curve; α and b are constants. From Eq. (6), the stiffness $dS_{\theta\theta}/dE_{\theta\theta}$ during loading shows a linear relationship to the circumferential stress as:

$$Y_{inc} = \frac{dS_{\theta\theta}}{dE_{\theta\theta}} = a(S_{\theta\theta} + b) \tag{7}$$

where Y_{inc} is incremental Young's modulus between the circumferential loading stress $S_{\theta\theta}$ and the no-load state stress. Since the no-load state stress is assumed negligible in this study, Y_{inc} represents the stiffness of the esophageal wall during the loading stress and a is the slope of the $Y_{inc} - S_{\theta\theta}$ curve.

3) Stiffness Softening Coefficient (SSC) and Stiffness Recovery Coefficient (SRC)

SSC is defined as the ratio of Y_{inc} at maximum stress value of cycle 1 during loading in S2 series to that in S1 series. SSC reflects the degree of stiffness loss caused by stress softening of the esophageal wall after cyclic loading in the S1 series.

SRC is defined as the ratio of Y_{inc} at maximum stress value of cycle 1 during loading in RE series to that in the S2 series. SRC reflects the degree of stiffness recovery of the esophageal wall after KCl activation.

2.8. Histology

The routine histology slides were stained with hematoxylin-eosin and Masson Trichrome staining. Hematoxylin-eosin staining was used to observe general histological changes and measurement of tube thickness. The Masson staining was used to visualize muscle and collagen and evaluate the tissue integrity after tube separation.

2.9. Statistical analysis

Data are presented as Mean ± SE. For comparing the body weight, blood glucose level and thickness of the esophageal wall, *t*-test analysis was used to test difference between DM and Sham groups. For comparing stored energy recovery, stiffness, stiffness loss and stiffness recovery, two-way ANOVA analysis was used for each pressure with the factors, 1: different tubes and 2: two dif-

ferent groups. The Tukey test was used for post hoc analysis. Linear regression analysis was used to analyze the association between the SSC and SRC of different tubes at different maximum pressures with blood glucose level at the end of experiment. Differences were considered statistically significant if $p < 0.05$. All analyses were done using the software package Sigma Stat v3.5 (SPSS Inc., USA).

3. Results

3.1. Basic data and histology

The Sham rats gained weight continuously whereas the DM rats maintained a relatively stable weight throughout the experiment (Table 1). The blood glucose level was relatively stable in the Sham group whereas the blood glucose level increased more than 3-fold for the DM group (Table 1). At end of experiment, the body weight was significantly lower and blood glucose was significantly higher in the DM group compared to the Sham group (Fig. 2, Body weight: $t = -5.464$, $P < 0.01$; Glucose: $t = 11.082$, $P < 0.001$). Muscle layer thickening was evident in the DM group (Fig. 2, $t = 4.861$, $P < 0.01$). Furthermore, tissue integrity after tube separation was well kept (data not shown).

3.2. Contraction induced by KCl

Fig. 3 shows typical KCl activation curves obtained from the intact (Fig. 3a), mucosa-submucosa (Fig. 3b) and muscle (Fig. 3c) tubes in the Sham and DM groups. KCl generated a significant muscle contraction in Sham esophagus with a sharp pressure increase up to 2.1 kPa in the intact (Fig. 3a), 1 kPa in the mucosa-submucosa (Fig. 3b) and 1.5 kPa in the muscle (Fig. 3c) tubes. For DM the pressure only increased up to 1.1 kPa in the intact (Fig. 3a) and 0.8 kPa in muscle (Fig. 3c) tubes. No change was observed in the mucosa-submucosa tube after KCl activation (Fig. 3b).

Table 1
Body weight (g) and blood glucose (mmol L^{-1}).

Times	D 1	D 3	D 4	W1	W 2	W 3	W 4	W5	W6	W7	W8
	Body weight (g)										
Sham	280.7 ± 22.7	294.6 ± 22.6	300.8 ± 22.6	308.3 ± 22.9	318.6 ± 25.8	330.5 ± 25.4	339.9 ± 26.1	348.1 ± 24.8	358.2 ± 27.2	364.7 ± 27.1	371.8 ± 27.6
DM	278.2 ± 27.6	266.1 ± 28.1	265.1 ± 27.2	272.7 ± 30.1	276.2 ± 35.0	276.8 ± 40.9	273.7 ± 44.0	271.0 ± 46.4	272.3 ± 47.6	269.0 ± 49.4	273.9 ± 52.3
P (*t*-test)	>0.8	<0.05	<0.01	<0.01	<0.01	<0.01	<0.01	<0.01	<0.01	<0.01	<0.01
	Glucose level (mmol L^{-1})										
Sham	5.97 ± 0.85	6.63 ± 0.36	6.80 ± 0.40	6.75 ± 0.58	6.44 ± 0.72	6.33 ± 0.57	6.28 ± 0.53	6.17 ± 0.26	6.46 ± 0.53	6.14 ± 0.56	6.66 ± 0.95
DM	5.75 ± 1.31	>22	>22	>22	>22	>22	>22	>22	>22	>22	23.58 ± 4.74
P (*t*-test)	>0.6	<0.01	<0.01	<0.01	<0.01	<0.01	<0.01	<0.01	<0.01	<0.01	<0.01

Notes: D: day, W: week. From Day 1 to week 7, the blood glucose level was measured by One-Touch blood glucose meter. When the blood glucose level is over 22 mmol L^{-1}, the monitor shows HHH. The blood glucose level at terminal of experiment (week 8) was measured by Auto Chemistry Analyzer.

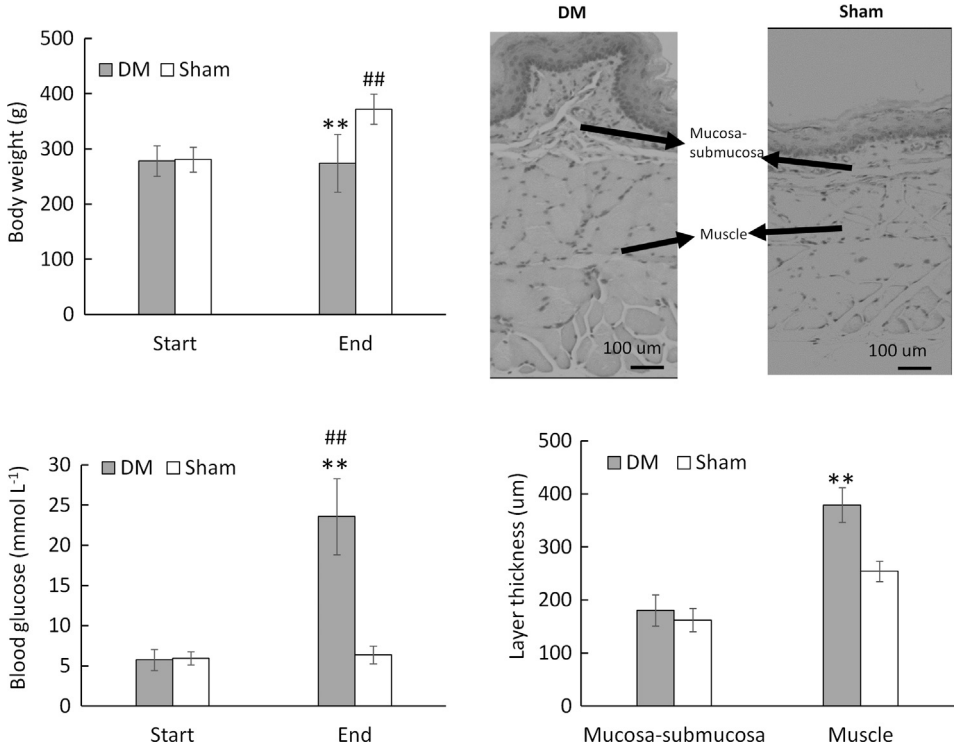

Fig. 2. Body weight, blood glucose and esophageal layer thickness. At end of experiment, the body weight of the Sham group was increased (top of left) and blood glucose level of DM group was increased (bottom of left) compared with that at the start of experiment. Furthermore, the body weight was lowest (top of left) and blood glucose was highest (bottom of left) in the DM group. Compared with the Sham group, the muscle layer of the DM group was thickest. Compared with start: $^{\#\#}$ $P < 0.01$; Compared with Sham group: ** $P < 0.01$.

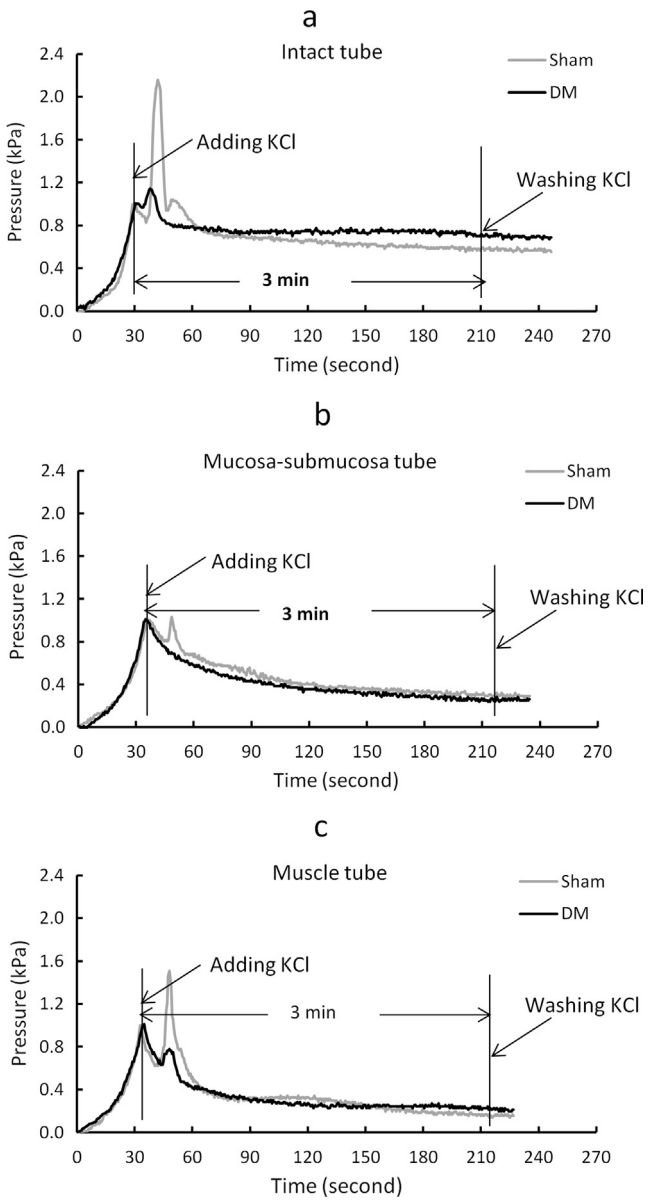

Fig. 3. Typical pressure curves after inflating the lumen to reach 1 kPa with KCl activation in Sham and DM esophagus. a: Intact esophagus tube; b: Mucosa-submucosa tube; c: Muscle tube.

3.3. Loss and recovery of storage energy

Fig. 4 shows loss and recovery of storage energy in the intact esophagus of Sham (top) and DM (bottom) groups. Results from mucosa-submucosa and muscle tubes are shown in Supplement Fig. 1. The difference between the area of the first cycle and fifth cycle of S2 represents viscoelastic softening. The difference between the area of the first cycle of S1 and the first cycle of S2 represents irreversible stress softening. The difference between the area of the first cycle of RE and the first cycle of S2 represents recovery of stored energy after activation of KCl. The data showed that the energy stored in the intact esophagus tube and the separated tubes was lost in both the DM group and the Sham group after S1 (Fig. 5). In the Sham group, energy loss in the intact esophagus and the separated tubes could be restored during RE (Fig. 5, q values from 3.826 to 4.861, $P < 0.05$), whereas it was not in the DM group (Fig. 5).

3.4. Stiffness of the esophagus tubes

Fig. 6 shows the effect of diabetes on stiffness in the intact (top), mucosa-submucosa (middle) and muscle (bottom) tubes at maximum pressure of 0.5 kPa. Results at maximum pressure of 1.0 and 2.0 kPa are shown in Supplement Fig. 2. The two curves on the left side of each graph are the stress-strain curves of the loading phase (Cycle1) in S1 of Sham and DM groups obtained from the different esophageal tubes. The inserting figure in each graph are the Young's modulus at the maximum stress level (Cycle1) of Sham and DM groups obtained from the different esophageal tubes. The intact esophagus and muscle tube was significantly stiffer in the DM group than in the Sham group (intact tube: $q = 3.717$; $P < 0.05$; muscle tube: $q = 5.012$, $P < 0.01$). Furthermore, the muscle tube was stiffer in the DM group at maximum pressure of 1.0 kPa, and 2.0 kPa when comparing the Y_{inc} at the maximum stress level of 2.8 and 5.6 kPa (See Supplement Figs. 2–3, $P < 0.05$).

3.5. SSC and SRC

Fig. 7 shows the comparison of SSC and SRC between Sham and DM groups for intact, mucosa-submucosa and muscle tubes. The stiffness of the muscle tube was lost more in the DM group than in Sham group when the maximum inflation pressure was 0.5 kPa ($q = 5.714$, $P < 0.001$). In comparison with the Sham group, the stiffness recovery in intact esophagus and muscle tubes was significantly altered in DM group (Intact tube: q values from 4.127 to 7.371, $P < 0.01$; Muscle tube: q values from 3.295 to 6.621, $P < 0.05$, $P < 0.01$).

3.6. Association between the SSC and SRC with blood glucose level at the end of experiment

The glucose level was associated positively with SSC and negatively with SRC. The significance was found for the glucose level with SSC of muscle tube and SRC of intact and muscle tubes at different maximum pressures. Fig. 8 shows the association between the glucose level with SSC of muscle tube at maximum pressure of 0.5 kPa (top figure: $F = 8.695$, $P = 0.012$), SRC of intact esophagus (middle figure) and muscle tube (bottom figure) at maximum pressure of 0.5 kPa (Intact esophagus tube: $F = 32.686$, $P < 0.001$; Muscle tube: $F = 17.083$, $P = 0.001$).

4. Discussion

In this study, results from the sham group confirmed that the stress softening of the esophagus was reversible, and the loss of passive stiffness was recoverable after KCl-induced contraction. However, for the STZ-induced diabetic group, the recovery of stress softening of the esophagus including the recovery of energy and stiffness was significantly altered, and the stiffness of the intact esophagus and muscle tube was increased. Furthermore, the stiffness loss and recovery of esophagus were associated with the blood glucose level.

Up to date, diabetes-induced histomorphological and biomechanical remodeling of the GI tract including the esophagus have been extensively studied (Zhao and Gregersen, 2016; Zhao et al., 2017). Increased esophageal wall stiffness has been demonstrated in the human diabetic esophagus (Frokjaer et al., 2007), in animal models of the type I diabetes (Yang et al., 2004, 2006) and the type II diabetes (Zhao et al., 2007a). This study further confirmed that diabetes increased esophageal stiffness. Furthermore, recovery of stress softening in the esophagus was significantly altered in the diabetic rats. Two factors are important for esophageal stress softening recovery, i.e., muscle contractility and wall stiffness. In this

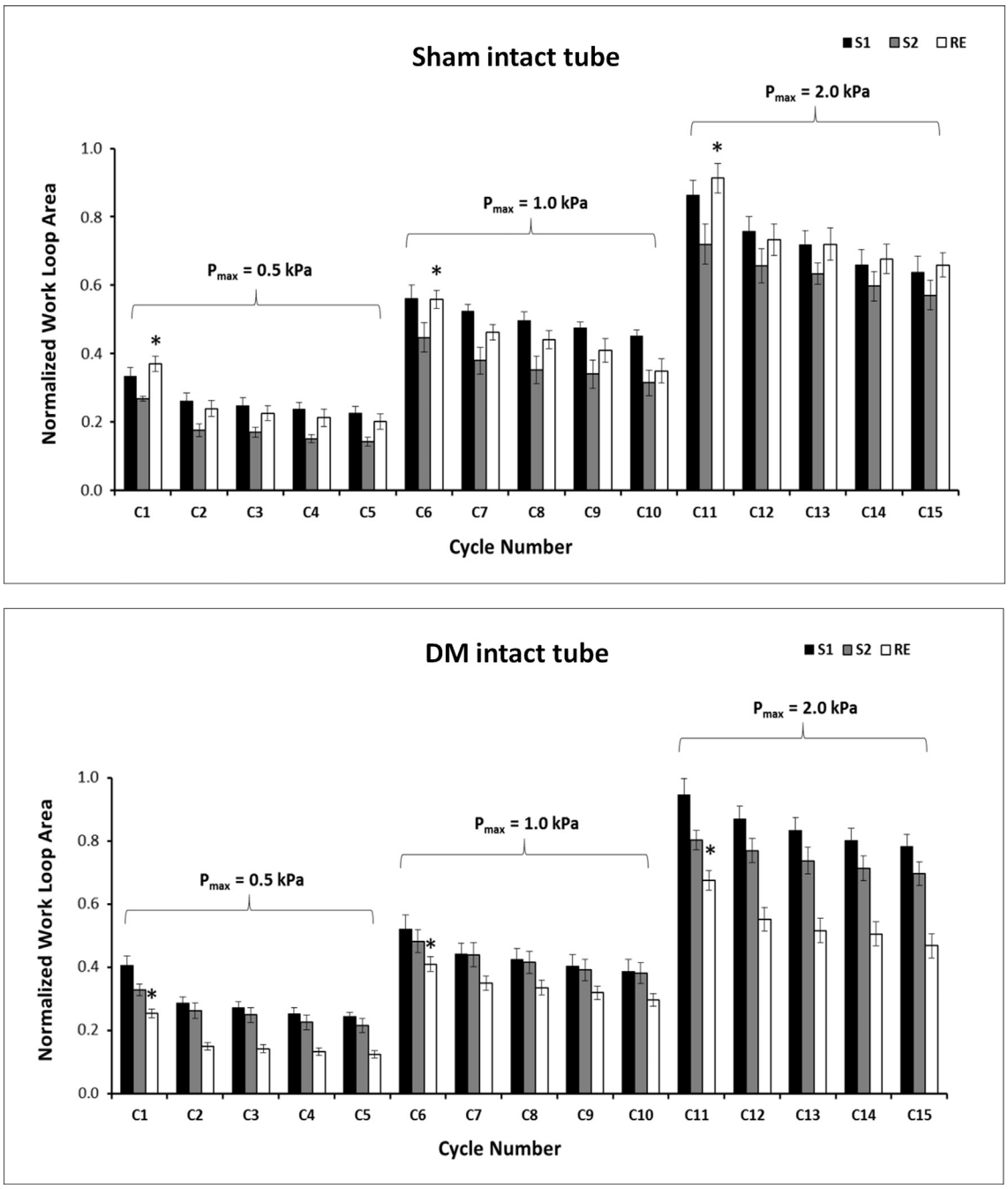

Fig. 4. Loss and recovery of storage energy in intact esophagus of Sham (top) and DM (bottom) groups. The energy stored at different maximum pressures was lost both in the DM group and in the Sham group. After KCl activation, the energy loss could be restored in the Sham group whereas it was not in the DM group. Comparison between the area of the first Cycle of the S2 at each pressure level and the area of the first Cycle of the RE: *P < 0.05.

study, the KCl-activated muscle contraction was somehow inhibited in the diabetic esophagus (Fig. 3). KCI-activated muscle contraction likely reflects muscle contractility (Dai et al., 2003; Sarr et al., 2013). Therefore, it indicates that the muscle contractility might be impaired. Previous studies have demonstrated esophageal motility disorders in nearly half of diabetic patients with dysphagia (George et al., 2017). Diabetic esophageal motor disorders are associated with disturbed glucose homeostasis (Ohlsson et al., 2006). In the present study, we found that SSC positively and SRC negatively were associated with glucose level (Fig. 8). Therefore, in our study the disturbed glucose homeostasis likely impaired esophageal muscle function that contributes to or reflects diabetes-induced alteration of esophageal stress softening recovery. However, future glucose clamp studies (Frøkjaer et al., 2010) are needed to investigate whether the glucose level has direct effect on esophageal biomechanical remodeling including esophageal stress softening recovery. Furthermore, the increasing wall stiffness in diabetes (Frokjaer et al., 2007; Yang et al., 2004, 2006; Zhao et al., 2007a) may contribute to the alteration of esophageal stress softening recovery. It is well known that advanced glycation end products (AGEs) accumulates in tissues during diabetes (Singh et al., 2001), which is associated with diabetes-induced esophageal remodeling. On one hand, AGEs deposited in the esophageal wall may cause thickening of the basement mem-

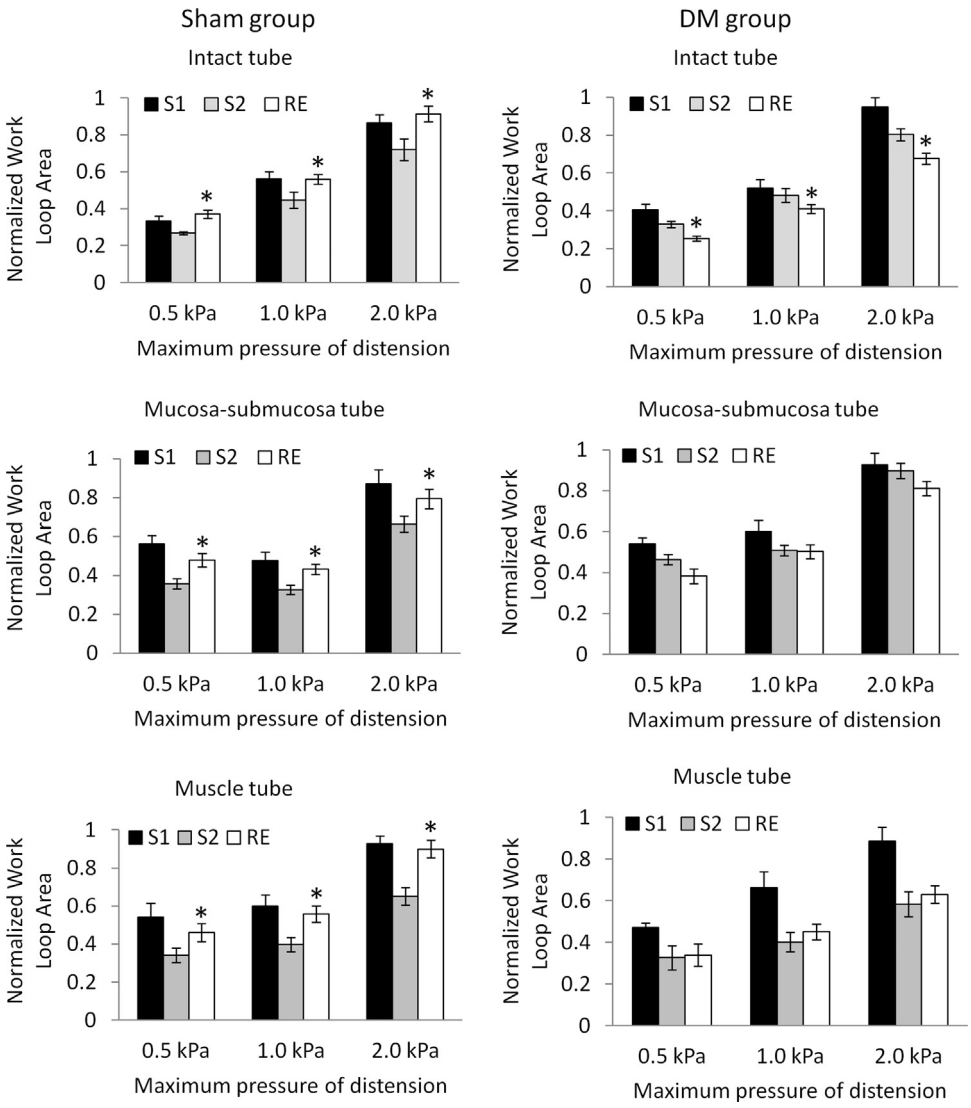

Fig. 5. The energy stored in the intact esophagus, mucosa-submucosa and muscle tubes: The energy was lost both in the DM group and in the Sham group. The energy loss could be restored in the Sham group after KCl activation whereas it was not in the DM group (Compared with S2: *P < 0.05). The normalized work loop area data refer to the first cycle for each Pmax shown in Fig. 4 for the intact esophagus and in Supplemental Fig. S1 for the two layers.

brane and the loss of the matrix elasticity through cross-linking of collagen (Reddy, 2004). On the other hand, AGEs may modify cellular functions of esophageal tissues through ligation of specific cell surface receptors (Bierhaus et al., 2005). Studies have shown that the formation of AGEs was related to the increased stiffness of the diabetic arterial wall (Sims et al., 1996). The expression of AGEs and receptor of AGEs (RAGE) in the diabetic GI wall including esophagus was up-regulated (Chen et al., 2012, 2015) and diabetes-induced morphology and biomechanical remodeling of the small intestine was closely associated with abnormal expressions of AGEs and RAGE (Zhao et al., 2013). The stiffness of the diabetic colon were significantly reduced by treatment with the glycation breaker ALT-711 (Siegman et al., 2016). Therefore, we believe that the abnormal accumulation of AGEs and the increased expression of RAGE and their receptors are closely related to diabetes-induced alteration of esophageal stiffening, stress softening and recovery.

The diabetes-induced esophageal morphological and biomechanical remodeling including the alteration of the esophageal stress softening likely affect esophageal physiological function by altering the structural and mechanical environment for nerve endings, mechanoreceptors, interstitial cajal cells (ICC), and muscles. Firstly, the remodeled structure and configuration of esophagus may alter the relative location of afferent nerve terminals in the esophageal wall (Zhao and Gregersen, 2016). Secondly, the remodeling of the stress and strain distribution and the increased stiffness of the esophagus likely change the micromechanical environment of the afferent nerve endings in the esophagus, affecting the reactivity to different stimuli in the esophagus. Thirdly, the recovery of esophageal stress softening could influence "self protecting" mechanism of the esophagus during esophageal expansion preceding primary peristaltic contractions. Although we did not study sensory-motor function of the esophagus and its direct relationship to the stress softening in the present study, the alteration of the esophageal stress softening by diabetes will one way or another affect the sensory-motor and contractile function of esophagus.

There are some limitations in present study. Firstly, we did not compare the esophageal stress softening at different stages of diabetes but only studied one time point (8 weeks). Secondly, the

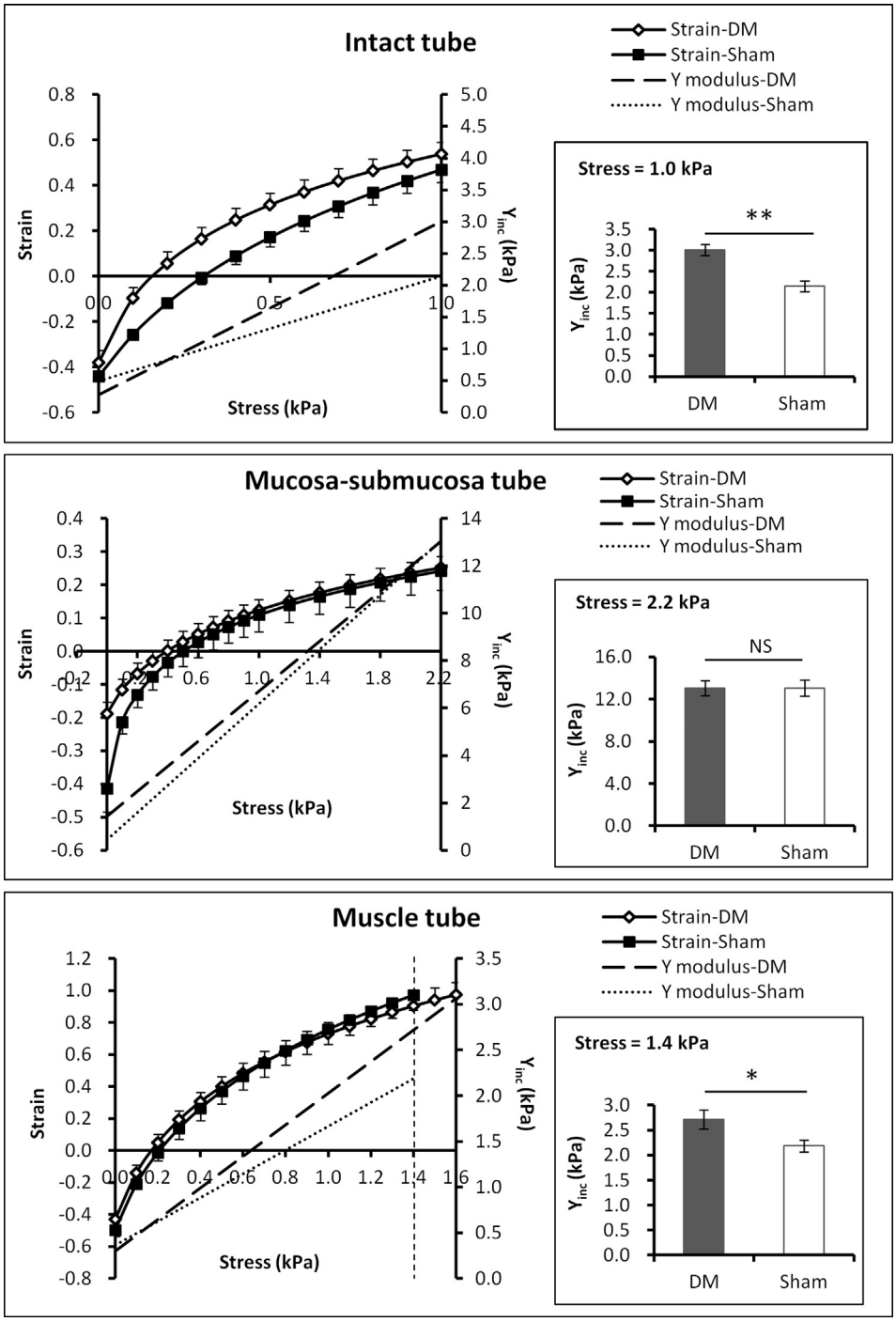

Fig. 6. Stiffness in intact esophagus (top), separated mucosa-submucosa (middle) and muscle (bottom) tubes at maximum pressure of 0.5 kPa. The intact esophagus and the muscle tube were stiffer in the DM group (Compared with sham: *P < 0.05, **P < 0.01). The two single dashed lines in the stress/strain graph on the left represent the mean for each group without standard error bars.

expectation of association between AGEs and RAGE with diabetes-induced alteration of stress softening and its recovery after stiffness lost is according to the data obtained from other studies. However, no direct evidence is presented in the present study. Thirdly, the anatomy of the esophagus differ somewhat between human and rat. The human esophagus contains striated muscle cells in the upper portion and smooth muscle cells in lower portion whereas the rat esophagus contains striated muscle cells along the entire length. However, the overall function is the same and significant differences between animal and human physiology have not been found (Goyal and Chaudhury, 2008). Fourthly, swine model is likely better than rat model to provide an approximation of human tissues and structures. However, in order to be comparable with our previous studies (Jiang et al, 2014, 2017; Yang et al, 2004, 2006), we decided to use rat model in the present study. Furthermore, rat esophageal samples are small, easy to handle, and have

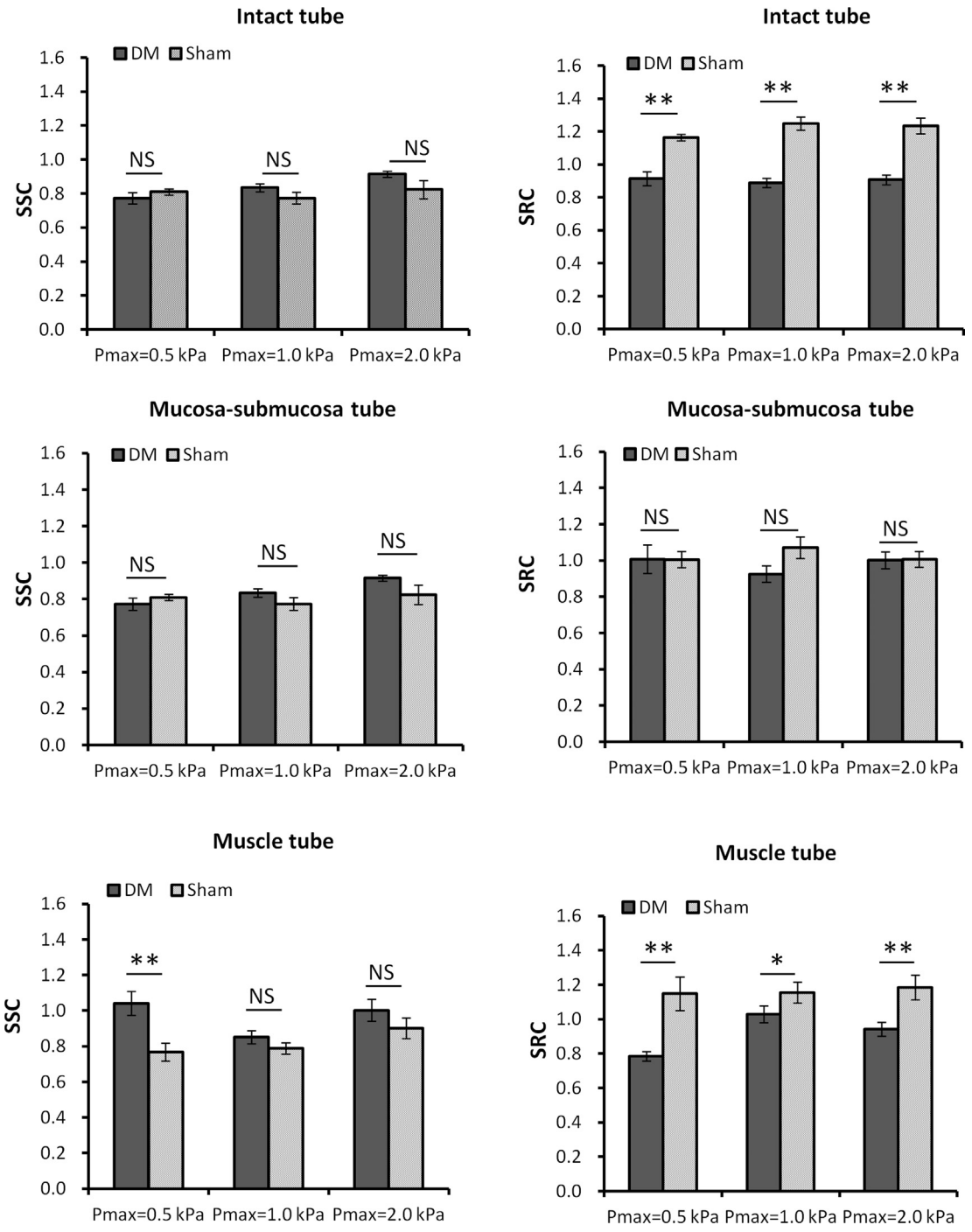

Fig. 7. Comparison of SSC and SRC between Sham and DM groups for intact esophagus, separated mucosa-submucosa, and muscle tubes. The muscle tube SSC was biggest in the DM group at maximum inflation pressure of 0.5 kPa (**P < 0.01). Compared with the Sham group, the SRC in intact esophagus and muscle tube were significantly smaller in the DM group (*P < 0.05, **P < 0.01).

a sufficiently small size for the tissue to survive in the physiological solution aerated with O_2 and CO_2 in the organ bath. Finally the blood glucose values are very tight for the sham, and very high for the DM, there are few blood glucose values between 7 and 20 mmol L^{-1}. Missing these values may somehow affect the correlations calculated in Fig. 8. Further research is needed to overcome these limitations.

In conclusion, the energy and stiffness loss recovery induced by stress softening was significantly smaller whereas the stiffness was significantly bigger in diabetic intact esophagus and separated muscular tube. This is the first study on the effect of diabetes on reversible stress softening and adjustable passive stiffness in the esophageal tissue. In addition to previous studies on diabetes-induced morphological and biomechanical remodeling, this study

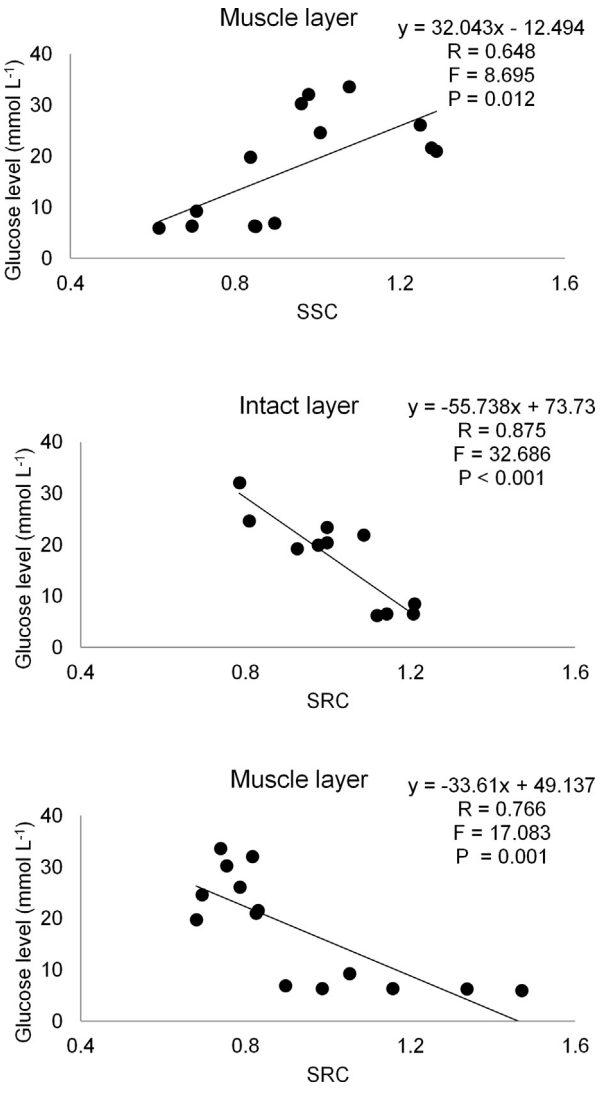

Fig. 8. The association between the glucose level with SSC of muscle tube (top figure), SRC of intact esophagus (middle figure) and muscle tube (bottom figure) at maximum pressure of 0.5 kPa. Positive association between glucose with SSC and negative association between glucose with SRC were found ($P < 0.05$, $P < 0.01$).

fills a gap about diabetes-induced esophageal time-history related biomechanical remodeling.

Declaration of Competing Interest

All authors report no conflicts of interest in this work..

Acknowledgements

This study was partially supported by a grant from Chongqing Science and Technology Commission (cstc2013kjrcljrccj10003), China; National "111 Plan" Base (B06023), China and Karen Elise Jensen Foundation, Denmark.

Author contribution

HJ performed the animal experiments, analyzed data, prepared manuscript including figures and tables. JZ analyzed histological data, wrote and revised manuscript, and provided partial funding support. DL performed mechanical data analysis and revised the manuscript. GW and HG designed and supervised the study, revised the manuscript and provided partial funding support. All authors reviewed the final version of the manuscript.

Appendix A. Supplementary material

Supplement figure 1: Supplement figures 1-1 and 1-2 show loss of and recovery of esophageal storage energy from mucosal-submucosal tube (Supplement figure.1-1) and muscular tube (Supplement figure.1-2) of esophagus of Sham (top) and DM (bottom) groups. The difference between the area of the first cycle and fifth cycle of S2 represents viscoelastic softening. The difference between the area of the first cycle of S1 and the first cycle of S2 represents irreversible stress softening. The difference between the area of the first cycle of RE and the first cycle of S2 represents the recovery of stored energy after activation of KCl. For each segment of esophageal tissue, the hysteresis loop area values obtained in all cyclic loadings were normalized to the largest area value generated by the tissue in whole experiment, and then statistical analysis was performed. In each figure, the area of the first Cycle of the S2 at each pressure level and the area of the first Cycle of the RE are compared to reflect the recovery of stored energy ($^{*}P < 0.05$). The experimental results showed that the energy stored in the mucosa-submucosa and muscle tubes was lost both in the DM group and the Sham group. In the Sham group, energy loss in the mucosa-submucosa and muscular tubes could be restored, while it was not in the DM group. Supplement figure 2: Supplement figures 2-1 to 2-3 show the effect of diabetes on stiffness in esophageal intact (Supplement figure. 2-1), mucosa-submucosa (Supplement figure. 2-2) and muscle (Supplement figure. 2-3) tubes. The two curves on the left side of each graph are the stress-strain curves of the loading phase (Cycle1) in S1 of Sham group and DM group obtained from the esophageal intact, mucosa-submucosa, and muscular tubes (maximum pressure of 1.0 kPa and 2.0 kPa). The inserting figure in each graph are the Young's modulus of the loading phase (Cycle1) of Sham group and DM group at pressures of 2.0 kPa and 4.0 kPa obtained from the esophageal intact, mucosa-submucosa and muscle tubes. The stiffness of muscle layers at all pressures are significantly bigger in DM group than in Sham group ($P < 0.05$).Supplementary data to this article can be found online at https://doi.org/10.1016/j.jbiomech.2019.05.042.

References

Bierhaus, A., Humpert, P.M., Morcos, M., Wendt, T., Chavakis, T., Arnold, B., Stern, D. M., Nawroth, P.P., 2005. Understanding RAGE, the receptor for advanced glycation end products. J. Mol. Med. 83 (11), 876–886.

Chen, P.M., Zhao, J.B., Gregersen, H., 2012. Up-regulated expression of advanced glycation end-products and their receptor in the Small Intestine and Colon of Diabetic Rats. Dig. Dis. Sci. 57 (1), 48–57.

Chen, P.M., Gregersen, H., Zhao, J.B., 2015. Advanced glycation end-product expression is upregulated in the gastrointestinal tract of type 2 diabetic rats. World J. Diabet. 6 (4), 662–672.

Cho, N.H., Shaw, J.E., Karuranga, S., Huang, Y., Jda Rocha Fernandes, D., Ohlrogge, A. W., Malanda, B., 2018. IDF Diabetes Atlas: global estimates of diabetes prevalence for 2017 and projections for 2045. Diabetes Res. Clin. Pract. 138, 271–281.

Dai, Y., Liu, J.X., Li, J.X., Xu, Y.F., 2003. Effect of pinaverium bromide on stress-induced colonic smooth muscle contractility disorder in rats. World J. Gastroenterol. 9 (3), 557–561.

Frokjaer, J.B., Andersen, S.D., Ejskjaer, N., Funch-Jensen, P., Drewes, A.M., Gregersen, H., 2007. Impaired contractility and remodeling of the upper gastrointestinal tract in diabetes mellitus type-1. World J. Gastroenterol. 13 (36), 4881–4890.

Frøkjaer, J.B., Søfteland, E., Graversen, C., Dimcevski, G., Drewes, A.M., 2010. Effect of acute hyperglycaemia on sensory processing in diabetic autonomic neuropathy. Eur. J. Clin. Invest. 40 (10), 883–886.

Frøkjaer, J.B., Brock, C., Brun, J., Simren, M., Dimcevski, G., Funch-Jensen, P., Drewes, A.M., Gregersen, H., 2012. Esophageal distension parameters as potential biomarkers of impaired gastrointestinal function in diabetes patients. Neurogastroenterol. Motil. 24 (11), 1016–1024.

George, N.S., Rangan, V., Geng, Z., Khan, F., Kichler, A., Gabbard, S., Ganocy, S., Fass, R., 2017. Distribution of esophageal motor disorders in diabetic patients with dysphagia. J. Clin. Gastroenterol. 51 (10), 890–895.
Goyal, R.K., Chaudhury, A., 2008. Physiology of normal esophageal motility. J. Clin. Gastroenterol. 42 (5), 610–619.
Jiang, H., Liao, D., Zhao, J., Wang, G., Gregersen, H., 2014. Contractions reverse stress softening in rat esophagus. Ann. Biomed. Eng. 42 (8), 1717–1728.
Jiang, H., Liao, D., Zhao, J., Wang, G., Gregersen, H., 2017. Reversible stress softening in layered rat esophagus in vitro after potassium chloride activation. Biomech. Model. Mechanobiol. 16 (3), 1065–1075.
Ohlsson, B., Melander, O., Thorsson, O., Olsson, R., Ekberg, O., Sundkvist, G., 2006. Oesophageal dysmotility, delayed gastric emptying and autonomic neuropathy correlate to disturbed glucose homeostasis. Diabetologia 49 (9), 2010–2014.
Ratz, P.H., Berg, K.M., Urban, N.H., Miner, A.S., 2005. Regulation of smooth muscle calcium sensitivity: KCl as a calcium-sensitizing stimulus. Am. J. Physiol.-Cell Physiol. 288 (4), C769–C783.
Reddy, G.K., 2004. AGE-related cross-linking of collagen is associated with aortic wall matrix stiffness in the pathogenesis of drug-induced diabetes in rats. Microvasc. Res. 68 (2), 132–142.
Sarr, M., Sar, F.B., Ngom, S., Wele, A., Guèye, L., Cissé, F., Samb, A., Lobstein, A., 2013. Differential inhibition of agonists-induced tracheal contraction after in vitro enriched-extracts treatment. J. Physiol. Pathophysiol. 4 (3), 37–45.
Siegman, M.J., Eto, M., Butler, T.M., 2016. Remodeling of the rat distal colon in diabetes: function and ultrastructure. Am. J. Physiol.-Cell Physiol. 310 (2), C151–C160.
Sims, T.J., Rasmussen, L.M., Oxlund, H., Bailey, A.J., 1996. The role of glycation cross-links in diabetic vascular stiffening. Diabetologia 39 (8), 946–951.
Singh, R., Barden, A., Mori, T., Beilin, L., 2001. Advanced glycation end-products: a review. Diabetologia 44 (2), 129–146.
Yang, J., Zhao, J., Zeng, Y., Gregersen, H., 2004. Biomechanical properties of the rat oesophagus in experimental type-1 diabetes. Neurogastroenterol. Motil. 16 (2), 195–203.
Yang, J., Zhao, J., Liao, D., Gregersen, H., 2006. Biomechanical properties of the layered oesophagus and its remodelling in experimental type-1 diabetes. J. Biomech. 39 (5), 894–904.
Zhao, J., Liao, D., Gregersen, H., 2007a. Biomechanical and histomorphometric esophageal remodeling in type 2 diabetic GK rats. J. Diabetes Complications 21 (1), 34–40.
Zhao, J., Jorgensen, C.S., Liao, D., Gregersen, H., 2007b. Dimensions and circumferential stress-strain relation in the porcine esophagus in vitro determined by combined impedance planimetry and high-frequency ultrasound. Dig. Dis. Sci. 52 (5), 1338–1344.
Zhao, J., Chen, P., Gregersen, H., 2013. Morpho-mechanical intestinal remodeling in type 2 diabetic GK rats–is it related to advanced glycation end product formation? J. Biomech. 46 (6), 1128–1134.
Zhao, J., Gregersen, H., 2016. Diabetes-induced mechanophysiological changes in the esophagus. Ann. N. Y. Acad. Sci. 1380 (1), 139–154.
Zhao, M., Liao, D., Zhao, J., 2017. Diabetes-induced mechanophysiological changes in the small intestine and colon. World J. Diabet. 8 (6), 249–269.